Groundwater

Case Study/

Septic Return Flow Pathlines, Endpoints, and Flows Based on the Urban Miami–Dade Groundwater Model

by Miguel E. Valencia[1], Michael C. Sukop[2], Grace Oldfield[3], Angela Montoya[4], Virginia Walsh[4], Jayantha Obeysekera[5], Samantha Barquin[6], Elizabeth Kelly[7], Katherine Hagemann[8], Aliza Karim[6], and Oscar F. Guzman[9]

Abstract

Miami-Dade County (MDC) has over 112,000 septic systems, some of which are at risk of compromise due to water table rise associated with sea level rise. MDC is surrounded by protected water bodies, including Biscayne Bay, with environmentally sensitive ecosystems and is underlain by highly transmissive karstic limestone. The main objective of the study is to provide first estimates of the locations and magnitudes of septic return flows to discharge endpoints. This is accomplished by leveraging MDC's county-scale surface-groundwater model using pathline analysis to estimate the transport and discharge fate of septic system flows under the complex time history of groundwater flow response to pumping, canal management, storms, and other environmental factors. The model covers an area of 4772 km^2 in Southeast Florida. Outputs from the model were used to create a 30-year (2010 to 2040) simulation of the spatial–temporal pathlines from septic input locations to their termination points, allowing us to map flow paths and the spatial distribution of the septic flow discharge endpoints under the simulated conditions. Most septic return flows were discharged to surface water, primarily canals 52,830 m^3/d and Biscayne Bay (5696 m^3/d), and well fields (14,066 m^3/d). Results allow us to identify "hotspots" to guide water quality sampling efforts and to provide recommendations for septic-to-sewer conversion areas that should provide most benefit by reducing nutrient loading to water bodies.

[1]Corresponding author: Department of Earth and Environment, Florida International University, 11200 SW 8th Street, Miami, FL 33199; mvale095@fiu.edu
[2]Department of Earth and Environment and Institute of Environment, Florida International University, 11200 SW 8th Street, Miami FL, 33199; sukopm@fiu.edu
[3]University of Dayton, 300 College Park, Dayton, OH 45469; graceoldfield33@gmail.com
[4]Miami-Dade Water and Sewer Department, 3071 SW 38th Avenue, Miami, FL 33146; angela.montoya@miamidade.gov; walshv@miamidade.gov
[5]Sea Level Solution Center in Institute of Environment, Florida International University, 11200 SW 8th Street, Miami, FL 33199; jobeysek@fiu.edu
[6]Miami Waterkeeper, P.O. Box 141596, Coral Gables, FL 33114; samantha@miamiwaterkeeper.org; aliza@miamiwaterkeeper.org
[7]Environmental Resource Division, Public Works Department, Martin County Board of County Commissioners, 2401 SE Monterey Road, Stuart, FL 34996, United States; ekelly@martin.fl.us
[8]City of San Rafael, 1400 Fifth Avenue, San Rafael, CA 94901; kate.hagemann@cityofsanrafael.org
[9]Department of Earth and Environment, Florida International University, 11200 SW 8th Street, Miami, FL 33199; oguzm013@fiu.edu

Article impact statement: Estimation of septic system effluent discharge endpoint locations and flows in Miami-Dade County, Florida, USA with particle tracking analysis.

[Correction added after first online publication on 12 September 2024; Copyright line has been updated.]

Received February 2023, accepted July 2024.

doi: 10.1111/gwat.13435

Introduction

Septic systems produce a number of contaminants, such as nutrients, pathogens (bacteria, virus, protozoa, helminths), human pharmaceuticals and personal care products (antibacterial agents, detergent metabolites) (Lusk et al. 2017), and any other substance a septic system user might dispose of in a tub, sink, or toilet. These can cause environmental degradation or illness if they reach surface water bodies or groundwaters. Using the terminology of, for example, Hughes and White (2016) and others, we refer to the water that moves directly to the aquifer from the septic system as septic return flow. Adequate septic system performance relies on an adequate residence time (Humphrey et al. 2015; Iverson et al. 2015) and an unsaturated treatment zone beneath the system's leach field to permit aerobic nitrification processes (USEPA 1999) and provide pathogen removal (Cogger et al. 1988, Figure 1). Sources of nitrogen and phosphorus in urban groundwater include septic systems, leaky sewer systems, treated and unintentional wastewater discharges, use of fertilizers, and landfill effluents (O'Driscoll et al. 2010).

Rising water tables in response to sea level rise and their implications for septic systems are a challenge in Southeastern Florida (Miami-Dade County 2018; Lusk 2022), other coastal areas in the United States (Manda et al. 2015; Vorhees et al. 2022), and around the globe.

The main objective of the study is to provide first estimates of the locations and magnitudes of septic flows to discharge endpoints. While previous studies in Miami-Dade County (Chin 2020; Miami-Dade County 2018) have looked at the county via large-scale mass balances and treat septic effluents as nonpoint sources, this is the first known attempt to explicitly track septic effluents in MDC based on a groundwater flow model, and few similar studies are known (e.g., Buszka and Reeves 2021). While particle tracking is frequently used to identify groundwater vulnerability (e.g., Klaas et al. 2017; Fiore and Colarullo 2023) and contributing areas of wells and coastal discharge areas determined using particle tracking sometimes include septic discharges (e.g., Sham et al. 1995; Barlow 1997; Masterson et al. 1997; Brawley et al. 2000; Robinson and Reay 2002; Morgan et al. 2007; Walter 2008), there appear to be few studies that exploit forward particle tracking from septic return flow sources.

This study was conducted to estimate the fate of septic return flows in terms of their ultimate discharge locations and flows by computing potential flow paths of septic effluents in MDC. Because the distribution of septic discharges and other variables relevant to the groundwater (e.g., water supply pumping and sea level) have changed over time in the past and are expected to continue to change in the future, the model that our work is based on is transient and looks 30 years into the future from 2010. Sea level is assumed to rise 15 cm over that period. This is expected to have some effect on the flowpaths of septic effluents, but given the numerous uncertainties and approximations involved in the simulation and our desire to make first estimates of approximate septic discharge endpoint locations and flows, we view our results as a hybrid of current and future conditions.

Study Site

MDC in Southeastern Florida includes barrier islands adjacent to the Atlantic Ocean and the larger mainland portion of the County, which are separated by Biscayne Bay (Figure 2). MDC is generally low-lying with an average elevation of 1.83 m above sea-level (Chao et al. 2021), and this leads to widespread shallow water tables that are rising in some areas of the County at rates similar to sea level rise (Sukop et al. 2018). The County has more than 112,000 residential septic systems (Miami-Dade County 2018), some of which were put into place prior to regulation, under less stringent regulations, and/or in areas where the groundwater level has increased over time. The design of these septic systems did not consider possible reductions of unsaturated zone thickness with time due to rising sea level, which can compromise their functionality.

Due to the slowly rising water table and superimposed rapid short-term rises in response to rainfall, it is estimated that 64% of the County's septic systems are periodically compromised, which is considered to be when there are less than 2 ft (approximately 0.6 m) separation from the water table, due to storms or wet years (Miami-Dade County 2018). By 2040, many will be too close to the water table at least part of the year to provide adequate wastewater treatment (Miami-Dade County 2018). When a septic system leach field becomes submerged, the film-flow filtration and aerobic treatment processes characteristic of the unsaturated zone are potentially lost and wastewater is directly discharged to groundwater without adequate treatment (Lusk et al. 2017).

Despite this risk of contamination due to compromised septic systems, septic-to-sewer conversion has been slow to proceed in MDC because of high cost. The cost of connecting about 83,000 septic-served properties to the County's sewer system is approximately \$3.3 billion (Miami-Dade County 2018). Even in areas that the County has identified as priorities, homeowners themselves are frequently reluctant to pay connection fees and the additional monthly fees.

Geology and Hydrogeology

MDC is underlain by the epikarstic surficial Biscayne Aquifer, which is one of the world's most productive aquifers, with transmissivities exceeding 28,000 m^2/d in some areas (Fish and Stewart 1991). Figure 2 shows the location of the study area in Florida and its elevation. The Atlantic Coastal Ridge is an elevated region near the coast that is interrupted in various places by low-lying "Transverse Glades" that were ancestral drainages and have been largely converted to dug drainage canals. These canals act as primary drainages and capture flows from inside the topographic divides that define their basins (Cooper and Lane 1987). The Biscayne Aquifer

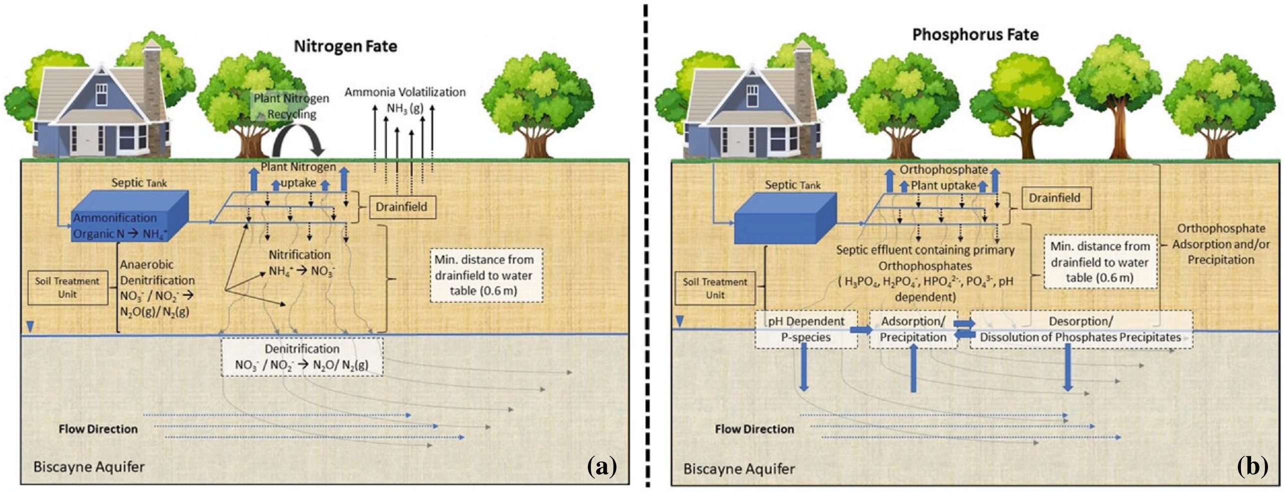

Figure 1. Possible nitrogen (a) and phosphorus (b) fate in septic system effluents, modified after Lusk et al. (2017). Increase of the water table elevation can compromise nitrification due to anoxic conditions and phosphate adsorption capacity due to iron and manganese reduction. Less than 0.6 m of separation between the bottom of the leach field and the water table leads to classification as a compromised system while partial seasonal (or longer) submergence leads to classification as a failed system (Miami-Dade County 2018).

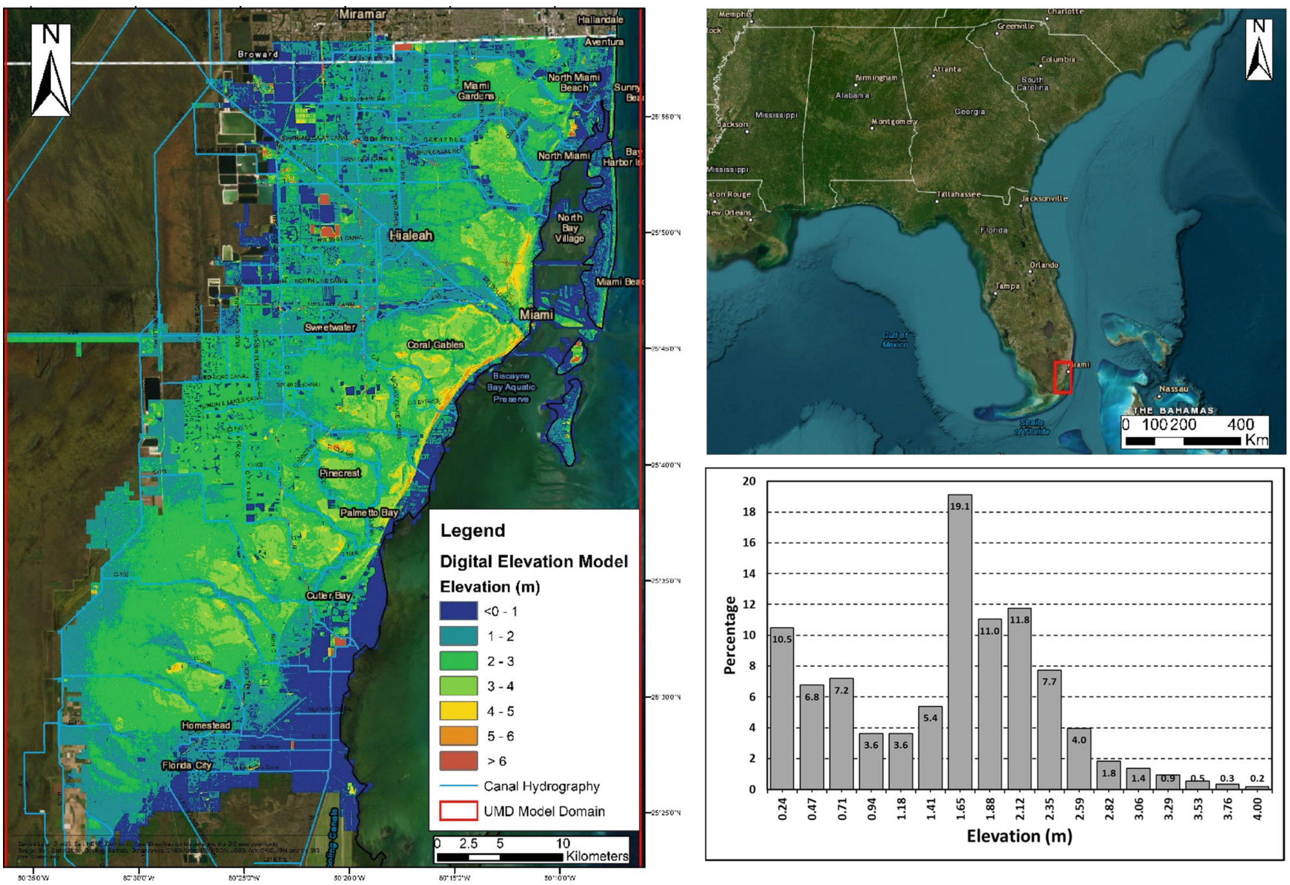

Figure 2. Map displaying the study area and Digital Elevation Model (DEM) with canal hydrography of Miami-Dade County (adapted from Miami-Dade County 2021); highest elevations on the map reflect landfills around the County (up to 71.2 m). Histogram (right, after Zhang 2011) shows distribution of NAVD88 elevations in the County. More than 95% of the land in the County (larger extent than shown in Figure 2) is less than 3 m NAVD88.

serves both municipal and private wells and owes its high transmissivity to its small (meter-sized) caverns (especially at bedding planes) and its vuggy nature in many places (Cunningham et al. 2006, 2009; Sukop and Cunningham 2014). The details and connectivity of such features are not resolvable at the County-wide scale and consequently, an equivalent porous medium approach is typically applied in models of the Biscayne Aquifer at that scale (e.g., Hughes and White 2016). While adequate permeability is necessary for proper function of septic systems, these extreme karst aquifer characteristics can prevent satisfactory treatment (USEPA 2001, 2002) and enable exceptional potential for solute and pathogen transport (Harvey et al. 2008; Renken et al. 2008).

Biscayne Bay suffers from fish kills and seagrass die-off related to nutrient and other forms of pollution. Most surface and groundwater in MDC is ultimately discharged to Biscayne Bay via an interconnected canal system and through groundwater discharge in the coastal area. The main sources of nutrient loading to canals are groundwater inflows and direct surface runoff.

Methods

Existing Groundwater Model

The Urban Miami-Dade (UMD) comprehensive surface-water/groundwater model developed by the U.S. Geological Survey (USGS) (Hughes and White 2016) has been serving a *de facto* role as a model of record in Southeast Florida. We leverage this model to compute the pathlines in this paper. The Miami-Dade surface/groundwater model is a three-layer, three-dimensional transient model that operates at a daily time step with a total of 10,958 daily stress periods representing 30 years. It simulates groundwater heads across its 189-row by 101-column domain using a grid resolution of 500 m × 500 m. Layer thickness, hydraulic conductivity and storage coefficients vary spatially as reported in Hughes and White (2016), and approximately reflect the distribution of recognized geologic units in the Biscayne Aquifer. Layer 1, which includes the water table, ranges from roughly 2 to 6 m in thickness, Layer 2 ranges from approximately 6 to 18 m, and Layer 3 ranges from 6 to 11 m, with all thicknesses increasing from west to east as described in Hughes and White (2016). A spatially variable specified flux boundary incorporated observed daily NEXRAD rainfall, estimated net agricultural and recreational water use, and septic system return flows as described in Hughes and White (2016).

The UMD model uses a 1-year warm-up period (January to December 1996) to mitigate the effect of the initial conditions prior to the calibration period from January 1997 through 2004, and is validated against data from January 2005 through December 2010. In the Base Future Conditions Case (Hughes and White 2016) that we used for our particle tracking simulations, the model is extended to future conditions from 2010 to 2040 by twice repeating most of the inputs using the 1996 to 2010 data, but including a 0.15 m sea level rise (equivalent to 5 mm/year) applied linearly over the 30-year simulation period; this sea level rise rate is consistent with data from the Virginia Key tide gauge, indicating an average rise of over 0.10 m since 1994 (4.8 mm/year, Compact 2015). Also, 2010 pumping rates were used for the future conditions (Hughes and White 2016). The Miami-Dade surface/groundwater model contains historical time-dependent land use-/land cover-based estimates of evapotranspiration and impervious areas, historical flows at primary water control structures, municipal, agricultural, and recreational groundwater pumping, septic system returns, and canal cross-sections for more than 1000 unique canal reaches.

Hughes and White (2016) provide a detailed description of the UMD model and its limitations related to the numerous model assumptions. Nonetheless, this model remains the best available tool for comprehensive ground-surface water simulation in MDC. Model output enables uses of MODPATH for particle tracking as we describe here.

Particle Tracking

MODPATH (Pollock 2012) is the principal tool used to leverage the pre-existing coupled ground-surface water model for the estimation of septic discharge fate via particle tracking; ModelMuse, ArcGIS, and Python were used for pre-/post-processing. It was assumed that a particle represents a flow of water equal to the septic return flow in the cell in which the particle originated. This is an approximation as it ignores mixing along the flow path and as a result produces a point discharge location. This may be a good approximation when the discharge location is a well, but is less appropriate where the discharge location is a canal or stream where the discharge would be spread out along a reach of the stream/canal. It is a further approximation that all septic return flows in a cell are represented by a particle starting at a single location in the cell.

The conceptual framework we apply is similar to the new volume-weighted particle tracking method of Winston et al. (2018), which serves as the heart of the new USGS transport model. Particles that enter the flow domain at septic sources are weighted by the volume of septic water they represent. The movement of the particles is tracked to their sinks, where the tracked volume of septic water is discharged (along with any other water picked up along the way that discharges at the same sink). No calculations or claims about concentration are made in our simplified approach. We simply track the input volume of septic water to its discharge location at the tracked particle's sink.

The particle tracks themselves approximately represent flowlines similar to those on a flow net, and hence, they do not cross one another and, other than transport across them by transverse dispersion, the tracked water volume (and by extension its contained solute mass neglecting transformation or any other degradation) is expected to be conserved.

The solute mass "flow" entering via the septic discharge must equal the volumetric flow of those septic inflows times their concentration. If we assume that the concentration of all septic inflow is identical, then the solute mass flow is strictly proportional to the septic inflow itself. Further, neglecting any solute transformations, the solute input mass must be conserved.

The approach described in Winston et al. (2018) is far more complicated than what we need to address our principal interest here. We are strictly interested in the paths of the input particles (which are weighted to represent the septic flow and hence, the mass flow of septic solutes) rather than their dilution or other mixing with flows from other sources. This is because we are interested in the solute mass flow discharge rather than the concentration. Attenuation and degradation of the dissolved water constituents are not taken into consideration; only the paths and ultimate discharge endpoint locations of the septic return flows are estimated.

The 30-year (2010 to 2040) Base Future Conditions Scenario simulation (Hughes and White 2016) was run to generate the binary output files (Cell-by-Cell Flows and Heads) needed to run MODPATH Version 6 package (Pollock 2012). All the original parameters from the UMD model were retained for the simulations. Initial particle locations were obtained from the original model's 2010 septic return flow input file by placing one particle in each model cell with non-zero septic return flow. Accordingly, 3256 particles were released at the beginning of the particle tracking simulation (stress period 1); initial particle locations are shown in Figure 3. Each released particle has a unique ID and spatial location with a corresponding flow value that allowed the tracking of particles and their associated flow to their discharge endpoints.

Specific Yield and Transport Porosity

Transport or effective porosity (n_e) is an important variable that determines particle velocity ($\boldsymbol{v}$) via:

$$\boldsymbol{v} = \frac{\boldsymbol{q}}{n_e} \tag{1}$$

where $\boldsymbol{q}$ is specific discharge (Darcy flux). Transport porosity is notoriously difficult to estimate other than from transport experiments (Stephens et al. 1998; Worthington 2022), which are generally not available for most of MDC.

Numerous studies have used specific yield as an estimate of transport porosity in the Biscayne Aquifer (e.g., Merritt 1996; Langevin 2001, 2003; Hughes and White 2016). Hughes and White (2016) estimated specific yield from model calibration and this parameter is a potential source for an estimate of the effective porosity needed in MODPATH's algorithms for computing groundwater velocity. Specific yields for Layer 1 were estimated using a pilot point calibration process; specific yield kriging resulted in a "bulls-eye" pattern as shown in figures 29 and 41 of Hughes and White (2016). The mean of Layer 1 specific yields obtained in the USGS's model calibration is 0.339 with a standard deviation of 0.081. In the UMD model, this specific yield was used as the transport porosity for the SWI2 package, and was also adopted for use in MODPATH particle tracking in this investigation. In MODPATH, Layers 2 and 3 were assigned constant transport porosity of 0.2 as used in other studies (Merritt 1996, 1997; Langevin 2001, 2003; Chin et al. 2010; Lohmann et al. 2012).

In some cases (e.g., Renken et al. 2008; Shapiro et al. 2008), the use of the specific yield as an estimate of transport porosity this appears to be a poor approximation that might grossly overestimate transport porosity and thereby underestimate the transport velocity. However, there is evidence that the appropriate transport porosity depends on the timescale of the transport process (Worthington et al. 2019; Worthington 2022). For short-term transport processes such those considered by Shapiro et al. (2008) and Renken et al. (2008), dominated by touching-vug flow zones representing high-velocity transport paths, the appropriate transport porosity can be a small fraction of the total porosity. For long-duration transport problems, the transport porosity appears to approach the total porosity (Worthington et al. 2019; Worthington 2022). Given that our interest is in transport on timescales generally greater than a year, transport porosities based on specific yields, which lie between the small estimated transport porosities from short term measurements and the total porosity, likely represent an appropriate approximation.

Septic Return Flows

As described in Hughes and White (2016), UMD septic return flows were computed for 3 times (1990, 2000, 2010) and then applied for the following decade (e.g., the 1990 estimate was applied for the 1990 to 1999 period) in the warmup/calibration/verification model run. They estimated septic system locations from data compiled by the Florida Department of Health based on tax records and a modeled probability that a parcel has a septic system (Hall and Clancy 2009). These results were combined with 1990, 2000, and 2010 census data to estimate discharge from active septic systems based on population density. The septic system database estimated 112,280 septic systems in the onshore part of the UMD study area. Combined with mean population per household in each census block and an average discharge of 0.21 cubic meters per day (m^3/d) per person (Marella 2004), total discharge to septic systems in the onshore portion of the study area was estimated to be 30,240, 76,032, and 71,712 m^3/d in 1990, 2000, and 2010, respectively (Hughes and White 2016). The 2010 spatial distribution of estimated septic discharge in cubic meters per day per grid cell is shown in figure 20c of Hughes and White (2016), including about 4000 m^3/d septic discharge on the barrier island, which is not included in the onshore totals above. Including the barrier island flows, the onshore total would be 75,642 m^3/d as reported in the results. Septic return flows were held steady at 2010 levels and spatial distributions in the Base Case Future UMD simulation that we use in our application of the particle tracking simulations.

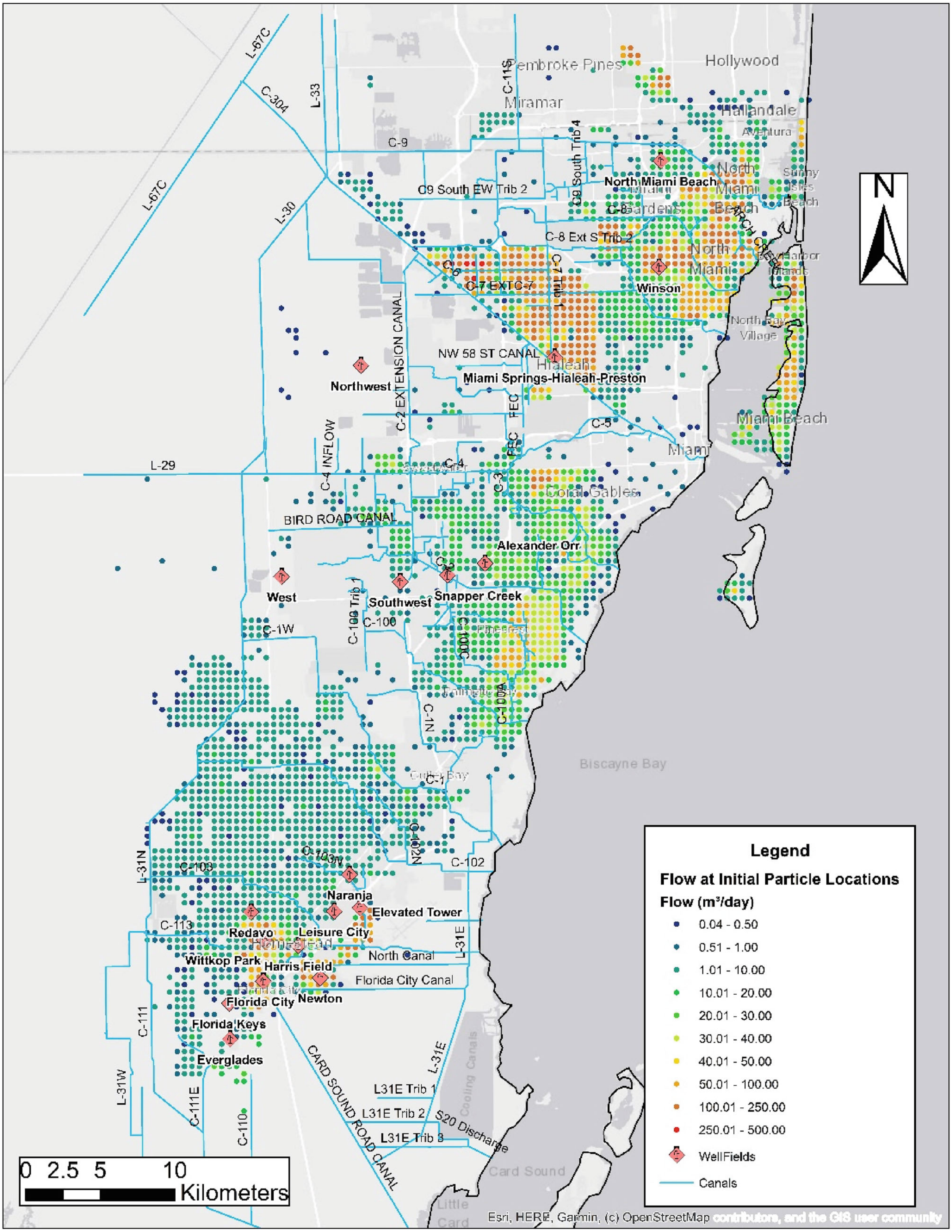

Figure 3. Map showing initial particle locations and septic return flow magnitudes (m^3/d) for the particle tracking simulation. Highest septic flows red, low flows blue, modified after Hughes and White (2016).

The location and status of septic systems is difficult to determine and few highly accurate databases exist. Differences between the estimates in Figure 3 and the County's current updated septic GIS layer (data source: Miami-Dade County 2022) may be due to differences in population density in the different areas, differences in septic deployment and abandonment, and septic-to-sewer conversion since the time the UMD model was created.

Results

Spatial–temporal pathlines with termination points were generated, allowing the mapping of estimated flow paths and the spatial distribution of estimated septic flow discharge endpoints. Septic return flow recharge locations based on UMD input data were used as starting points (Figure 3) for the 30-year particle tracking simulations.

Hughes and White's (2016) report shows septic return flows for the onshore study area only, though the actual UMD model files as archived by USGS used estimated septic flows for the entire county including the barrier island of Miami Beach. Although local agencies anecdotally report that there are no septic systems on Miami Beach, the USGS approach to estimating septic discharges included flows on Miami Beach as shown in Figure 3. County reports (Miami-Dade County 2018, 2020) also show septic systems on Miami Beach and it is nearly certain that there once were many such systems. This discrepancy does not substantially affect our results or conclusions given that the emphasis is on mainland basins and canals that drain into Biscayne Bay, particularly the northernmost portions of the Bay where water quality impacts are greatest.

Discharge Endpoint Locations and Flows

Figure 4 shows the discharge endpoint for each simulated grid cell that had a septic return flow source. Simulated particles frequently descended at the beginning of the simulation, some reaching model Layers 2 and 3 but coming back to the upper layer when discharge endpoints were reached. Septic return flows in the model were discharged to endpoints in surface water (52,830 m^3/d), well fields (14,066 m^3/d), and directly to Biscayne Bay (5696 m^3/d).

Figure 5 shows the initial particle locations and the pathlines, which are colored to illustrate the time, in years, elapsed before endpoint discharge. The mean travel time for 90% of the pathlines, which reached their discharge endpoints during the 30-year simulation, was estimated to be about 8.5 years. These estimates are expected to be sensitive to the transport porosities used in the pathline simulation (see section on Specific Yield and Transport Porosity above). Ten percent of the particles were estimated to be still active after 30 years.

Septic flows, pathlines, and discharge endpoints as flows are shown in Figure 6. The average discharge flow for the termination points is about 23 m^3/d. The Miami Springs-Hialeah-Preston well fields capture a high density of high-flow-rate flow paths in the simulation.

Assessment of Simulated Discharge Endpoint Locations

Simulated discharge endpoint locations were analyzed by areas of interest, including drainage basins, canals, well fields, and the Bay itself. About 70% of the septic return flows terminated in canals, 19% in well fields, 7% directly in Biscayne Bay, and 4% of the flows terminated on the ocean side and other areas (Table 1).

Figure 7 shows the simulated distribution of discharge flows terminating in canals and near the Miami Springs-Hialeah-Preston production wells. Estimated discharges to canals, which accounted for 70% of the terminating septic return flows, were further analyzed by specific basin in the northernmost part of the county. Similar work assessing sources of total nitrogen (TN) and total phosphorus (TP) to groundwater was completed by Chin (2020) and was used for comparison with our findings.

Analysis of Simulated Discharges to Well Fields

Of the 19% of simulated total septic return flows estimated to terminate on well fields (Table 2), 49% was discharged to the Miami Springs-Hialeah-Preston (MS-HI-PP) production wells (termination points at this location are shown on Figure 7) followed by 14% at the Winson well field; remaining discharge percentages by well field are found on Table 2a.

Additionally, 2010 base-rate pumping from MDC wellfields was used to estimate the fractions of inflows to production wells that are estimated to come from simulated septic discharge flows (Table 2b). The MS-HI-PP wellfield had the highest simulated septic return inflow of 6903 m^3/d representing 2.6% of the total production well field's base-rate pumping; the remaining wellfields were estimated to capture less than 1% septic return flows as shown on Table 2.

Basin-wide Analysis of Septic Flow Discharges for Northern MDC

The basin-wide estimates that we present here are not specific to groundwater or canals, but rather represent an overall loading within boundaries of the basins. In our work, the C-7 basin is the area that had the highest number of estimated septic return flow termination points and associated discharges (19,324 m^3/d), which accounts for 49% of the total septic discharges among the four basins (Figure 7, Table 3).

We used average total canal flows from Chin (2020) to estimate the ratios of septic return flows to total flows coming from the northern MDC basins. This represents the proportions of canal flow comprised of septic effluent. The analysis yielded percentages of 1.0%, 3.9%, 1.8%, and 0.4% for the C-6, C-7, C-8, and C-9 canals, respectively (Table 4).

Discussion

Model results suggested that half of the particles reach their sinks in less than 4.9 years and septic-to-sewer conversions would be expected to yield potential water quality improvements in that timeframe for those particles.

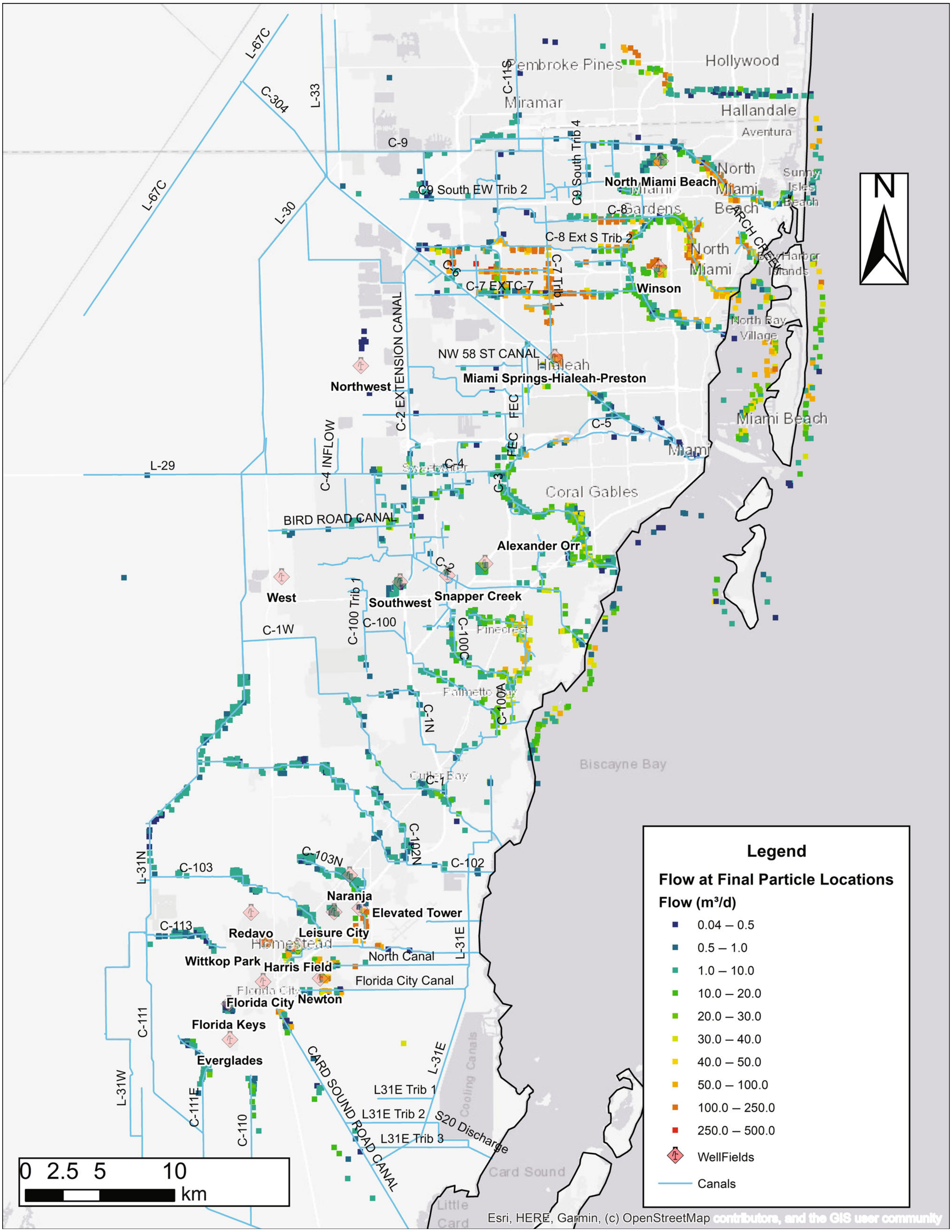

Figure 4. Septic discharge endpoints for the 30-year particle tracking simulation. Note that symbol overlap in some areas of high endpoint density – near well fields in particular – prevents many endpoints from being visible.

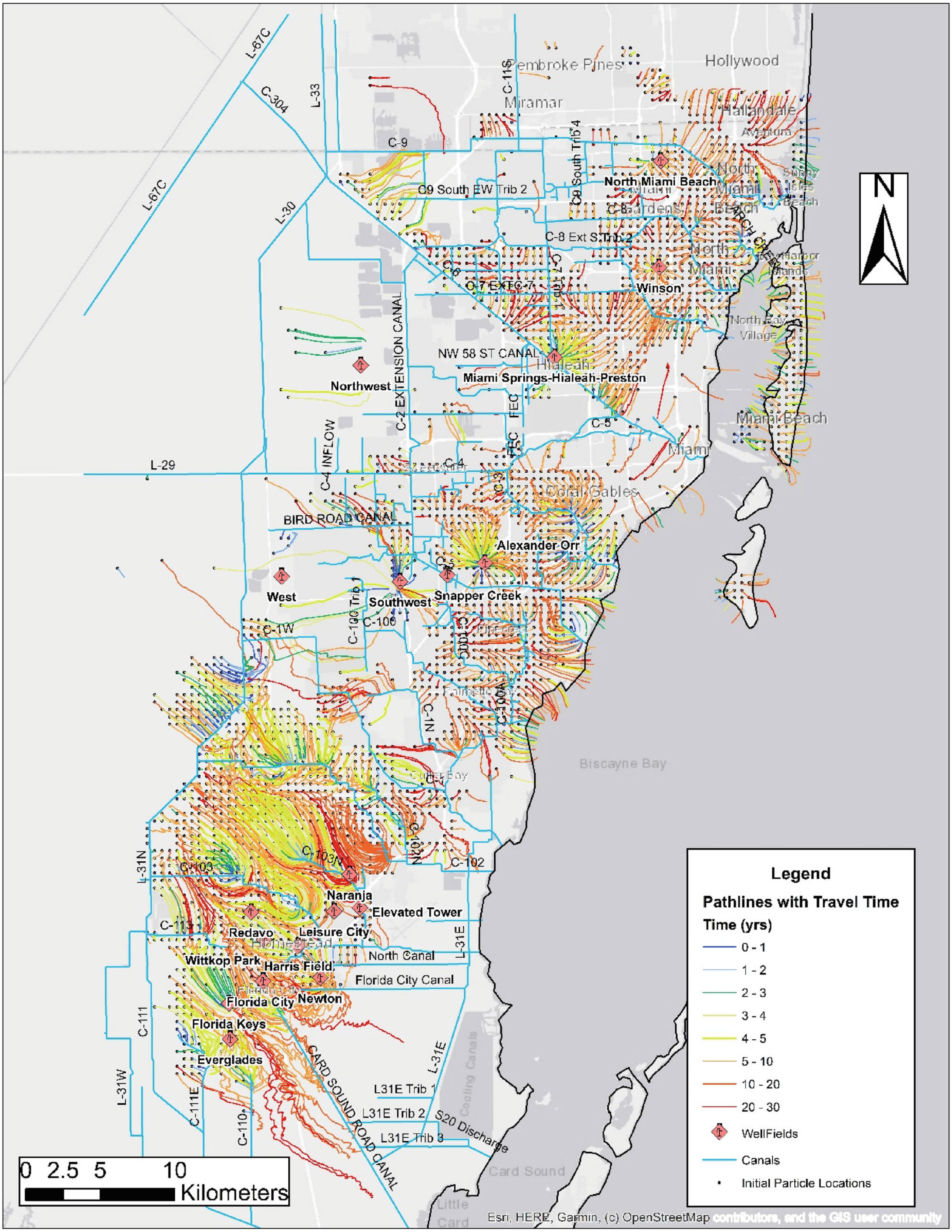

Figure 5. Map with initial particle locations and particle tracking times in years.

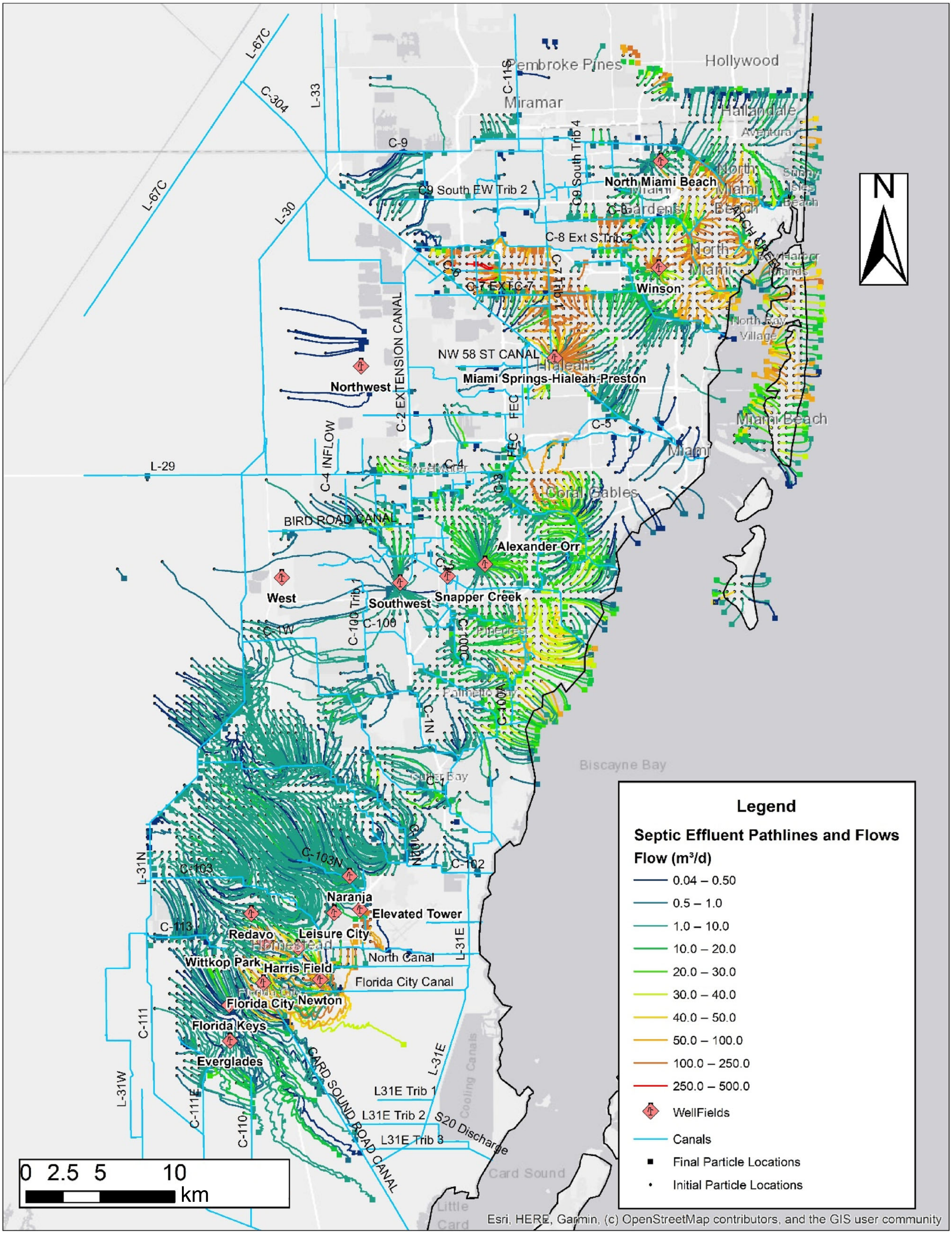

Figure 6. Map with flow color-coded simulated pathlines and endpoints.

Table 1
Overall Distribution of Septic Flow Fate

Endpoint Flows by Area of Interest		
Location	**Septic Endpoint Flow (m^3/d)**	**Percentage Distribution (%)**
Canals	52,830	70
Well fields	14,066	19
Biscayne Bay	5696	8
Ocean side	1747	2
Other	1303	2
Totals	75,642	—

Note: Pathline termination points falling within a distance of 500 m from a canal or well field was the criterion used to assign discharge to canals and well fields.

The remaining 1552 particles had longer discharge times (including 190 particles with discharge times longer than 30 years), and this suggests that near-term septic-to-sewer conversion in areas that contribute to those slower flows might require multiple years or decades to have an impact on receiving waters.

Some of the approaches and the resolution used to simulate processes in the underlying groundwater flow model may lead to overestimation of the flow of the septic discharge and the transport of its potential constituents. In particular, in suburban areas the model ignores potentially plentiful small domestic irrigation wells that might capture septic effluent. The model assumes that lawn irrigation in urban areas comes entirely from municipal water sources. In contrast, regional South Florida Water Management District models estimate that about 50% of lawn irrigation comes from domestic wells.

The 500-m grid UMD model represents canals and other features as occupying an entire grid cell. Under these circumstances, the entire cell containing a canal acts as a "drain" and potentially captures more particles over a larger area. Preliminary grid resolution studies on small selected areas suggest that in a spatially refined model with explicit representation of small domestic irrigation wells, particles that are very close to a canal (less than 30 m) are captured by the canal, while many particles are captured by these wells in a cell. Similarly, particles that are estimated to be captured by a public water supply well

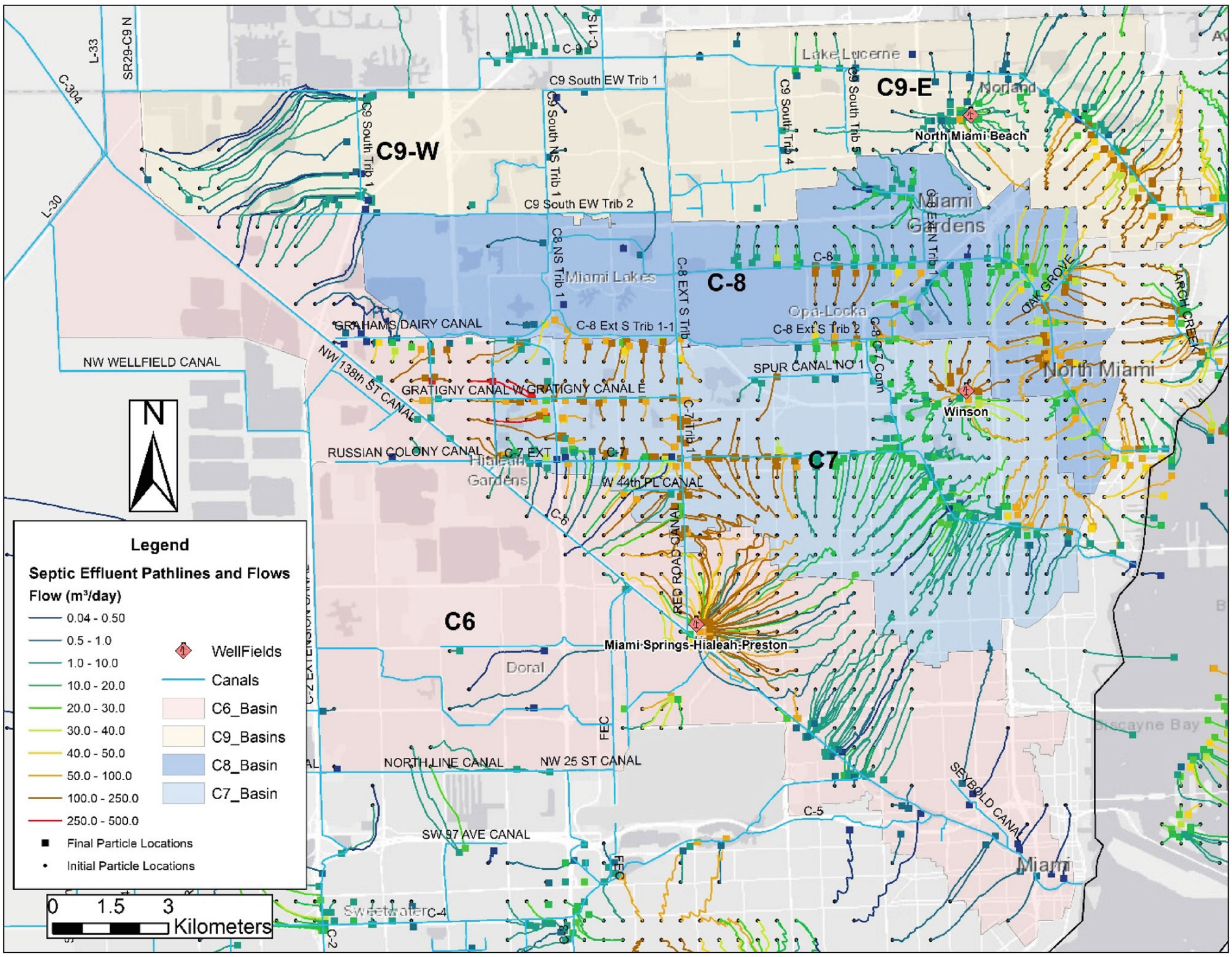

Figure 7. Map with MDC's northern basins and canals. Zoomed-in discharge points and particle pathlines near the Miami Springs-Hialeah-Preston production wells showing simulated septic flow discharge endpoint locations in canals, wellfields, and to the Bay.

Table 2
(a) Distribution of Simulated Septic Effluents Discharged to Well Fields. (b) Production Well Inflows from Septic Return Flows and 2010 Groundwater Pumping Rate (Referred to as Base Rate) from Hughes and White (2016)

(a) Endpoint Flows at Well Fields

Well Field	Septic Endpoint Flow (m^3/d)	Percentage Distribution (%)
Miami Springs-Hialeah-Preston	6903	49
Winson	2010	14
Wittkop	1223	9
A. Orr	1162	8
Other	1062	8
Harris	884	6
NMB	336	2
SW	310	2
FL Keys	177	1
Totals	14,066	—

(b) Septic Endpoint Flows and Percentage from Base Rate Pumpage

Well Fields	Septic Endpoint Flow (m^3/d)	Base Rate (m^3/d)	Percentage from Septic Endpoint Flows (%)
Miami Springs-Hialeah-Preston	6903	264,979	2.6
Alexander Orr	1162	151,416	0.8
South West	310	414,124	0.1

Table 3
Simulated Septic Effluent Distributions by Basins and Canals

Endpoint Flows Basins and canals

Basin	Septic Endpoint Flow (m^3/d)	Percentage	Canal	Septic Endpoint Flow (m^3/d)	Percentage
C-6	8952	23	C-6	5168	17
C-7	19,324	49	C-7	11,316	37
C-8	7326	18	C-8	8520	28
C-9	4163	10	C-9	5217	17
Totals	39,765	—	Totals	30,221	—

field, may instead be captured by domestic lawn irrigation wells. Fundamentally, a more refined grid that includes these wells and better resolves canals and pumping wells may turn weak lawn irrigation sink cells into stronger sink cells capable of capturing local groundwater. If whole-UMD-model simulations could be carried out at high resolution, canals and public supply wells might not play as significant a role in capturing flow from septic system returns as they do in the coarser model.

Table 4
Septic-Derived Fraction of Total Canal Flows per Basin, Total Canal Flow Data from Chin (2020).

Endpoint Flows Basins

Basin	Septic Endpoint Flow (m^3/d)	Total Canal Flow (m^3/d)	Percent
C-6	8952	855,360	1.0
C-7	19,324	492,480	3.9
C-8	7326	414,720	1.8
C-9	4163	993,600	0.4
Totals	39,765	2,756,160	—

The UMD model assumes agricultural irrigation needs can be represented as a negative recharge in the "GFB" package. In reality, agricultural producers extract water from wells that can also capture septic effluents. Experimental modeling of a selected agricultural area represented irrigation as wells and found that most simulated septic discharge was captured by the wells rather than the canals. Thus, contributions of septic discharges to canals might be lower than estimated in our work. Domestic and agricultural irrigation pumping may capture groundwater nutrients and transfer them to the root zone for uptake by plants and reduce overall loading of nutrients to regional water systems. Thus, our results may represent worst-case conditions for septic return flow fate in MDC.

Septic effluent distributions were also analyzed and compared, focusing on basins and canals in the northern part of the County. The C-7 basin was the area subject to the highest septic return flow with 49% of the total septic discharge among the four basins. Using a different approach based on septic system counts per basin from the Miami-Dade GIS portal, assuming that each of those systems serves a three-person household with per-capita loading of 284 L/d, and that TN and TP concentrations in system effluent are 50 and 5 mg/L, respectively, Chin (2020) estimated considerably different total septic return TN and TP than we would estimate based on septic return flows from the UMD model as shown in Table 5. The probabilistic and population-based approach to septic inflow estimation adopted by the USGS in the UMD model is primarily responsible for the differences in these estimates.

Conclusions

Coastal MDC has shallow and in some areas rising water tables, which pose risks to functionality of septic systems (Miami-Dade County 2018). Episodic water table rises in response to storms can also compromise septic system functionality and in severe cases, high water tables may reach the surface, causing and/or exacerbating flooding and carrying septic water constituents with them. Flooded drain fields and flooded septic tanks

Table 5
Comparison of Simulated Septic Effluent Distributions by Basins with Septic Load Distributions for TN and TP Reported by Chin (2020)

Basin	Percentage of Simulated Septic Endpoint Flow	Percentage of TN/TP Loading (Chin 2020)
C-6	23	10
C-7	49	43
C-8	18	25
C-9	10	22

potentially pose major health issues and need to be addressed with high priority.

Key outcomes of this study are (1) a particle tracking model of septic return flow discharge endpoints based on the UMD model from Hughes and White (2016), (2) an estimate of septic return flow discharge "hot-spots" in the County (Figure 4), and (3) comparison of model results with previous studies in northern MDC (Table 5), which has the highest septic return flow discharges and contributes to contamination of Biscayne Bay.

The 30-year (2010 to 2040) particle tracking simulation conducted in this study estimated the movement and discharge locations of septic return flows under the assumption that the septic discharge flow was steady throughout the simulated period. Most flows terminated on canals, well fields, and the Bay itself. Flows terminating in canals will ultimately be transported to and discharged to Biscayne Bay. Simulated pathline particles were also captured by municipal production wells. For flows estimated to terminate in well fields (19% of total septic return flows), only a small fraction of produced water is expected to be septic return flow and frequent County monitoring shows no evidence of impact either in wellfield monitoring wells or production wells. The highest estimated fraction of total flow from a production well field estimated to originate from septic return flows is 2.6%. Other, more local capture processes may be responsible for further reducing such loading to production wells as discussed above.

Acknowledgments

We thank the four anonymous reviewers and the editors Dr. Leonard Konikow, Dr. Charles Andrews, and Dr. Kenneth Bradbury for their helpful comments, which lead to substantial improvement of the manuscript. This material is based upon work supported by the National Science Foundation under Grant No. HRD-1852123. This grant was awarded to Florida International University as part of the Research Experiences for Undergraduates (REU) Site Program. This paper is a result of research funded by the National Oceanic and Atmospheric Administration National Centers for Coastal Ocean Science Competitive Research Program under award NA23NOS4690260-T1-01 to Florida International University. This is contribution number 1738 from the Institute of Environment at Florida International University.

Authors' Note

The authors do not have any conflicts of interest or financial disclosures to report.

DATA AVAILABILITY STATEMENT

The data that support the findings of this study are available from the corresponding author upon reasonable request.

References

Barlow, P.M. 1997. Particle-tracking analysis of contributing areas of public-supply wells in simple and complex flow systems, Cape Cod, Massachusetts. U.S. Geological Survey Water Supply Paper 2434, vi, 66 p., https://doi.org/10.3133/wsp2434.

Brawley, J.W., G. Collins, J.N. Kremer, C. Sham, and I. Valiela. 2000. A time-dependent model of nitrogen loading to estuaries from coastal watersheds. *Journal of Environmental Quality* 29, no. 5: 1448–1461. https://doi.org/10.2134/jeq2000.00472425002900050011x

Buszka, T.T., and D.M. Reeves. 2021. Pathways and timescales associated with nitrogen transport from septic systems in coastal aquifers intersected by canals. *Hydrogeology Journal* 29, no. 5: 1953–1964. https://doi.org/10.1007/s10040-021-02362-8

Chao, S.R., B. Ghansah, and R.J. Grant. 2021. An exploratory model to characterize the vulnerability of coastal buildings to storm surge flooding in Miami-Dade County, Florida. *Applied Geography* 128: 102413. https://doi.org/10.1016/j.apgeog.2021.102413

Chin, D.A. 2020. Source identification of nutrient impairment in North Biscayne Bay, Florida, USA. *Journal of Environmental Engineering* 146, no. 9: 04020101. https://doi.org/10.1061/(ASCE)EE.1943-7870.0001786

Chin, D.A., J.J. Iudicello, K.C. Kajder, P.M. Kelly, D.V. Porzilli, and H. Guha. 2010. Lake effect in wellhead protection. *Journal of Water Resources Planning and Management* 136, no. 3: 403–407. https://doi.org/10.1061/(ASCE)WR.1943-5452.0000032

Cogger, C.G., L.M. Hajjar, C.L. Moe, and M.D. Sobsey. 1988. Septic system performance on a Coastal Barrier Island. *Journal of Environmental Quality* 17, no. 3: 401–408. https://doi.org/10.2134/jeq1988.00472425001700030009x

Cooper, M., and J. Lane. 1987. An atlas of eastern Dade County surface water management basins. South Florida Management District, Resource Planning Department, Water Resources Division.

Cunningham, K.J., M.C. Sukop, H. Huang, P.F. Alvarez, H.A. Curran, R.A. Renken, and J.F. Dixon. 2009. Prominence of ichnologically influenced macroporosity in the karst Biscayne aquifer: Stratiform "super-K" zones. *Geological Society of America Bulletin* preprint, no. 2008: 1. https://doi.org/10.1130/B26392.1.

Cunningham, K.J., M.A. Wacker, E. Robinson, J.F. Dixon, and G.L. Wingard. 2006. A Cyclostratigraphic and Borehole Geophysical Approach to Development of a Three-Dimensional Conceptual Hydrogeologic Model of the Karstic Biscayne Aquifer, Southeastern Florida. U.S. Geological Survey Scientific Investigations Report 2005-5235, 69 p., plus CD. https://doi.org/10.3133/sir20055235.

Fiore, A.R., and S.J. Colarullo. 2023. Simulation of regional groundwater flow and advective transport of per- and polyfluoroalkyl substances, Joint Base McGuire-Dix-Lakehurst and vicinity, New Jersey, 2018. U.S. Geological Survey Open-File Report 2022–1112, 41 p., 2 pls. https://doi.org/10.3133/ofr20221112.

Fish, J.E., and M. Stewart. 1991. Hydrogeology of the surficial aquifer system, Dade County, Florida. U.S. Geological Survey Water-Resources Investigations Report 90-4108. https://doi.org/10.3133/wri904108.

Hall, P., and S.J. Clancy. 2009. Statewide inventory of onsite sewage treatment and disposal systems in Florida. Final Report. https://www.floridahealth.gov/environmental-health/onsite-sewage/research/ResearchReports/˙documents/0125-florida-inventory-ostds.pdf. (accessed May 23, 2023).

Harvey, R.W., D.W. Metge, A.M. Shapiro, R.A. Renken, C.L. Osborn, J.N. Ryan, K.J. Cunningham, and L. Landkamer. 2008. Pathogen and chemical transport in the karst limestone of the Biscayne aquifer: 3. Use of microspheres to estimate the transport potential of *Cryptosporidium parvum* oocysts. *Water Resources Research* 44, no. 8:1–12. https://doi.org/10.1029/2007WR006060

Hughes, J., and J. White. 2016. Hydrologic conditions in urban Miami-Dade County, Florida, and the effect of groundwater pumpage and increased sea level on canal leakage and regional groundwater flow (ver. 1.2, July 2016): U.S. Geological Survey Scientific Investigations Report 2014-5162, 175 p. https://doi.org/10.3133/sir20145162.

Humphrey, C., A. Finley, M. O'Driscoll, A. Manda, and G. Iverson. 2015. Groundwater and stream *E. coli* concentrations in coastal plain watersheds served by onsite wastewater and a municipal sewer treatment system. *Water Science and Technology* 72, no. 10: 1851–1860. https://doi.org/10.2166/wst.2015.411

Iverson, G., M.A. O'Driscoll, C.P. Humphrey, A.K. Manda, and E. Anderson-Evans. 2015. Wastewater nitrogen contributions to coastal plain watersheds, NC, USA. *Water, Air, & Soil Pollution* 226, no. 10: 325. https://doi.org/10.1007/s11270-015-2574-4

Klaas, D.K.S.Y., M.A. Imteaz, and A. Arulrajah. 2017. Development of groundwater vulnerability zones in a data-scarce eogenetic karst area using head-guided zonation and particle-tracking simulation methods. *Water Research* 122: 17–26. https://doi.org/10.1016/j.watres.2017.05.056

Langevin, C.D. 2003. Simulation of submarine ground water discharge to a marine estuary: Biscayne Bay, Florida. *Groundwater* 41, no. 6: 758–771. https://doi.org/10.1111/j.1745-6584.2003.tb02417.x

Langevin, C.D. 2001. Simulation of ground-water discharge to Biscayne Bay, Southeastern Florida. U.S. Geological Survey Water-Resources Investigations Report 00-4251, https://doi.org/10.3133/sir20125099.

Lohmann, M., E. Swain, J. Wang, and J.F. Dixon. 2012. Evaluation of effects of changes in canal management and precipitation patterns on salinity in Biscayne Bay, Florida, using an integrated surface-water/groundwater model. U.S. Geological Survey Scientific Investigations Report 2012–5099, 94 p. https://doi.org/10.3133/sir20125099.

Lusk, M.G. 2022. Public health threats of diminished treatment of onsite sewage. *The Lancet Planetary Health* 6, no. 9: e707–e708. https://doi.org/10.1016/S2542-5196(22)00191-7

Lusk, M.G., G.S. Toor, Y.-Y. Yang, S. Mechtensimer, M. De, and T.A. Obreza. 2017. A review of the fate and transport of nitrogen, phosphorus, pathogens, and trace organic chemicals in septic systems. *Critical Reviews in Environmental Science and Technology* 47, no. 7: 455–541. https://doi.org/10.1080/10643389.2017.1327787

Manda, A.K., M.S. Sisco, D.J. Mallinson, and M.T. Griffin. 2015. Relative role and extent of marine and groundwater inundation on a dune-dominated barrier Island under sea-level rise scenarios. *Hydrological Processes* 29, no. 8: 1894–1904. https://doi.org/10.1002/hyp.10303

Marella, R.L. 2004. Water withdrawals, use, discharge, and trends in Florida, 2000. U.S. Geological Survey Scientific Investigations Report 2004-5151. https://doi.org/10.3133/sir20045151.

Masterson, J.P., D.A. Walter, and J.G. Savoie. 1997. Use of particle tracking to improve numerical model calibration and to analyze ground-water flow and contaminant migration, Massachusetts military reservation, western Cape Cod, Massachusetts. *U.S. Geological Survey Water-Supply Paper* 2482: 50.

Merritt, M.L. 1997. Simulation of the water-table altitude in the Biscayne aquifer, southern Dade County, Florida, water years 1945-89. U.S. Geological Survey Water-Supply Paper 2458, 148 p., 9 pls. https://doi.org/10.3133/sir20125099.

Merritt, M.L. 1996. Assessment of saltwater intrusion in southern coastal Broward County, Florida. U.S. Geological Survey Water-Resources Investigations Report 96-4221, 133 p. https://doi.org/10.3133/sir20125099.

Miami-Dade County. 2022. MDC, DOH Septic System Layer Open Data Hub, 2022, https://gis-mdc.opendata.arcgis.com/. (accessed November 14, 2022).

Miami-Dade County. 2021. MDC, 2021: 5-ft DEM Open Data Hub, 2021, https://gis-mdc.opendata.arcgis.com/. (accessed November 14, 2022).

Miami-Dade County. 2020. Plan of Action Report - A Risk-Based Approach to Septic Systems Vulnerable to Sea Level Rise. https://www.miamidade.gov/mayor/library/memos-and-reports/2020/12/12.10.20-Septic-Systems-Vulnerable-to-Sea-Level-Rise-Plan-of-Action-Report.pdf. (accessed September 22, 2022).

Miami-Dade County. 2018. Septic Systems Vulnerable to Sea Level Rise: Final Report in support of Resolution No. R-911-16. https://www.miamidade.gov/green/library/vulnerability-septic-systems-sea-level-rise.pdf. (accessed August 09, 2022).

Morgan, D.S., S.R. Hinkle, and R.J. Weick. 2007. Evaluation of approaches for managing nitrate loading from on-site wastewater systems near La Pine, Oregon. U.S. Geological Survey Scientific Investigations Report 2007-5237, 66 p.

O'Driscoll, M., S. Clinton, A. Jefferson, A. Manda, and S. McMillan. 2010. Urbanization effects on watershed hydrology and in-stream processes in the southern United States. *Water* 2, no. 3: 605–648. https://doi.org/10.3390/w2030605

Pollock, D. 2012. User guide for MODPATH version 6 – A particle-tracking model for MODFLOW. U.S. Geological Survey Techniques and Methods s 6–A41, 58 p. https://doi.org/10.3133/tm6A41.

Renken, R.A., K.J. Cunningham, A.M. Shapiro, R.W. Harvey, M.R. Zygnerski, D.W. Metge, and M.A. Wacker. 2008. Pathogen and chemical transport in the karst limestone of the Biscayne aquifer: 1. Revised conceptualization of groundwater flow. *Water Resources Research* W08429: 44. https://doi.org/10.1029/2007WR006058

Robinson, M.A., and W.G. Reay. 2002. Ground water flow analysis of a mid-Atlantic outer coastal plain watershed, Virginia, U.S.A. *Groundwater* 40, no. 2: 123–131. https://doi.org/10.1111/j.1745-6584.2002.tb02497.x

Sham, C.H., J.W. Brawley, and M.A. Moritz. 1995. Quantifying septic nitrogen loadings to receiving waters: Waquoit Bay, Massachusetts. *International Journal of Geographical Information Systems* 9, no. 4: 463–473. https://doi.org/10.1080/02693799508902050

Shapiro, A.M., R.A. Renken, R.W. Harvey, M.R. Zygnerski, and D.W. Metge. 2008. Pathogen and chemical transport in the karst limestone of the Biscayne aquifer: 2. Chemical retention from diffusion and slow advection. *Water*

Resources Research 44, no. 8: 1–12. https://doi.org/10.1029/2007WR006059
Southeast Florida Regional Climate Change Compact. 2015. Southeast Florida regional climate change compact. https://southeastfloridaclimatecompact.org/wp-content/uploads/2023/10/2015-sea-level-projections.pdf. (accessed June 27, 2024).
Stephens, D.B., K.-C. Hsu, M.A. Prieksat, M.D. Ankeny, N. Blandford, T.L. Roth, J.A. Kelsey, and J.R. Whitworth. 1998. A comparison of estimated and calculated effective porosity. *Hydrogeology Journal* 6, no. 1: 156–165. https://doi.org/10.1007/s100400050141
Sukop, M.C., M. Rogers, G. Guannel, J.M. Infanti, and K. Hagemann. 2018. High temporal resolution modeling of the impact of rain, tides, and sea level rise on water table flooding in the Arch Creek basin, Miami-Dade County Florida USA. *Science of The Total Environment* 616–617: 1668–1688. https://doi.org/10.1016/j.scitotenv.2017.10.170
Sukop, M.C., and K.J. Cunningham. 2014. Lattice Boltzmann methods applied to large-scale three-dimensional virtual cores constructed from digital optical borehole images of the karst carbonate Biscayne aquifer in southeastern Florida. *Water Resources Research* 50, no. 11: 8807–8825. https://doi.org/10.1002/2014WR015465
USEPA. 2002. USEPA onsite wastewater treatment systems manual. https://www.epa.gov/sites/default/files/2015-06/documents/2004_07_07_septics_septic_2002_osdm_all.pdf. (accessed May 19, 2023).
USEPA. 2001. Source water protection practices bulletin managing septic systems to prevent contamination of drinking water. https://www.epa.gov/sites/default/files/2015-06/documents/2006_08_28_sourcewater_pubs_septic.pdf. (accessed May 19, 2023).
USEPA. 1999. Preliminary data summary of urban storm water best management practices. https://www.epa.gov/sites/default/files/2015-11/documents/urban-stormwater-bmps_preliminary-study_1999.pdf. (accessed May 19, 2023).
Vorhees, L., J. Harrison, M. O'Driscoll, C. Humphrey, and J. Bowden. 2022. Climate change and onsite wastewater treatment systems in the Coastal Carolinas: Perspectives from wastewater managers. *Weather, Climate, and Society* 1: 1287–1305. https://doi.org/10.1175/WCAS-D-21-0192.1
Walter, D.A. 2008. Use of numerical models to simulate transport of sewage-derived nitrate in a coastal aquifer, Central and Western Cape Cod, Massachusetts. Scientific Investigations Report.
Winston, R.B., L.F. Konikow, and G.Z. Hornberger. 2018. Volume-weighted particle-tracking method for solute-transport modeling: Implementation in MODFLOW–GWT. In *U.S. Geological Survey Techniques and Methods*, book 6, chap. A58, Reston, VA: U.S. Geological Survey.
Worthington, S.R.H. 2022. Estimating effective porosity in bedrock aquifers. *Groundwater* 60, no. 2: 169–179. https://doi.org/10.1111/gwat.13171
Worthington, S.R.H., A.E. Foley, and R.W.N. Soley. 2019. Transient characteristics of effective porosity and specific yield in bedrock aquifers. *Journal of Hydrology* 578: 124129. https://doi.org/10.1016/j.jhydrol.2019.124129
Zhang, K. 2011. Analysis of non-linear inundation from sea-level rise using LIDAR data: A case study for South Florida. *Climatic Change* 106, no. 4: 537–565. https://doi.org/10.1007/s10584-010-9987-2